Published in final edited form as:

Neurochem Res. 2008 May ; 33(5): 745–753. doi:10.1007/s11064-007-9490-y.

Kinetics of Human Serum Butyrylcholinesterase Inhibition by a Novel Experimental Alzheimer Therapeutic, Dihydrobenzodioxepine Cymserine

Mohammad A. Kamal, **Peter Klein**, **Weiming Luo**, **Yazhou Li**, **Harold W. Holloway**, **David Tweedie**, and **Nigel H. Greig**

[1]Department of Medical and Molecular BioSciences, Faculty of Science, University of Technology Sydney, Sydney, Australia

[2]Drug Design and Development Section, Laboratory of Neurosciences, Intramural Research Program, National Institute on Aging, National Institutes of Health, Gerontology Research Center, Baltimore, MD, USA

Abstract

Cholinergic loss is the single most replicated neurotransmitter deficiency in Alzheimer's disease (AD) and has led to the use of acetylcholinesterase inhibitors (AChE-Is) and unselective cholinesterase inhibitors (ChE-Is) as the mainstay of treatment. AChE-Is and ChE-Is, however, induce dose-limiting adverse effects. Recent studies indicate that selective butyrylcholinesterase inhibitors (BuChE-Is) elevate acetylcholine (ACh) in brain, augment long-term potentiation, and improve cognitive performance in rodents without the classic adverse actions of AChE-Is and ChE-Is. BuChE-Is thereby represent a new strategy to ameliorate AD, particularly since AChE activity is depleted in AD brain, in line with ACh levels, whereas BuChE activity is elevated. Our studies have focused on the design and development of cymserine analogues to induce selective time-dependent brain BuChE inhibition, and on the application of innovative and quantitative enzyme kinetic analyses to aid selection of drug candidates. The quantitative interaction of the novel inhibitor, dihydrobenzodioxepine cymserine (DHBDC), with human BuChE was characterized. DHBDC demonstrated potent concentration-dependent binding with BuChE. The IC50 and specific new kinetic constants, such as KT50, PPC, KT1/2 and RI, were determined at dual substrate concentrations of 0.10 and 0.60 mM butyrylthiocholine and reaction times, and are likely attainable in humans. Other classical kinetic parameters such as Kia, Kma, Vma and Vmi were also determined. In synopsis, DHBDC proved to be a highly potent competitive inhibitor of human BuChE in comparison to its structural analogue, cymserine, and represents an interesting drug candidate for AD.

Keywords

Alzheimer's disease; Butyrylcholinestrase; Acetylcholinesterase; Anticholinesterase; Cymserine; Phenserine; Bisnorcymserine; Enzyme inhibition kinetics; New kinetic constants

Dedicated to Professor Moussa Youdim, Dept. Pharmacology, Technion, Haifa, Israel, in celebrating 45 years in scientific research focused on drug discovery and 30 years at Technion.

Introduction

Mounting evidence suggests that butyrylcholinesterase (BuChE: EC 3.1.1.8), a glycoprotein enzyme belonging to the serine esterases family [1], has an important role in Alzheimer's disease (AD) [2–4], the most common dementia in the elderly [5, 6]. BuChE is found in plasma and various compartments within the body, and is widely distributed in the nervous system [1, 2]. Whereas its function remains to be fully elucidated, it catalyses the hydrolysis of numerous endogenous substances, including choline esters and the growth hormone secretagogue, octanoyl ghrelin [1, 2, 7, 8]. Although associated with glial cells, in human brain, BuChE is additionally expressed in neuronal somata and their proximal dendrites in areas affected by AD, such as in the amygdala, hippocampus and thalamus [1, 9, 10]. By contrast, acetylcholinesterase (AChE: EC 3.1.1.7), the enzyme classically associated with catalyzing the hydrolysis of the neurotransmitter acetylcholine (ACh), is found in the somata and axons [9, 10]. The survival and 'normality' of the brain of AChE nullizygote (AChE −/−) versus normal (AChE +/+) mice, together with the distinct and overlapping distribution patterns of AChE- and BuChE-positive neurons, raises the likelihood that BuChE is involved in neural function [3, 11, 12], for example co-regulation of cholinergic and non-cholinergic neurotransmission [1–3, 11, 12].

The over-expression of BuChE in hippocampus and temporal cortex, in AD compared to normal subjects, at a time when AChE is reduced in line with a substantial decline in markers of the cholinergic system [13], suggests that an imbalance exists between the two primary enzyme subtypes that regulate ACh in the AD brain [2]. Recent studies indicate that selective BuChE inhibitors (BuChE-Is) elevate brain extracellular levels of ACh, augment long-term potentiation, which is considered to be the cellular basis of learning and memory in vertebrates, and improve cognitive performance in rodents [3, 14] without the classic adverse actions of either AChE-Is or unselective cholinesterase inhibitors (ChE-Is). AChE-Is (donepezil) and ChE-Is (rivastigmine and galantamine) are currently the mainstay of AD treatment, but induce dose-limiting adverse effects [5]. Hence, selective BuChE inhibition thereby represents an interesting new strategy to ameliorate AD, particularly since BuChE readily cleaves ACh and co-localizes in high amounts with the classical pathological hallmarks of AD and may be involved in the molecular events underpinning disease progression [1, 2, 15, 16].

Our studies have focused on the design and development of novel 'drug-like' compounds on the backbone of the natural product alkaloid and classical anticholinesterase, physostigmine (eserine) (Fig. 1B), to induce time-dependent brain BuChE inhibition [17]. Our design of 'cymserine' analogues [18] (Fig. 1D, E) provided lipophilic reversible inhibitors with these features with high brain penetration to target AD [3]. Herein, we characterize the quantitative interaction of the novel inhibitor, dihydrobenzodioxepine cymserine (DHBDC) [19–21] (Fig. 1A), with BuChE by combining the classic Ellman method [22] to measure the cleavage of choline esters with innovative and quantitative enzyme kinetic analyses to both aid selection of drug candidates and define target concentrations for future translational studies [23–26].

Experimental procedures

Materials

Butyrylthiocholine iodide (BuSCh, was used as a substrate), 5,5′-dithiobis(2-nitrobenzoic acid) (DTNB as a coloring reagent), and 1,5-bis(4-allyldimethyl-ammoniumphenyl) pentan-3one dibromide (BW284C51) were obtained from Sigma (St Louis, MO, USA) while human serum BuChE was obtained from a local blood bank (unit # 8599114; ARCBS Sydney; ORhD positive). DHBDC ((±)-4,5-dihydro-2,5-methyl-1,3-benzodioepin-7-yl N-(4′-isopropylphenyl)-carbamate) was synthesized as reported earlier [19–21], and was prepared as a racemate (Fig. 1A).

Assay of BuChE Activity

BuChE activity was measured at 25°C by the Ellman method [22]. The assay mixture contained BuSCh, 0.25 mM DTNB, 0.05 mM BW284C51 (a classic selective, potent and irreversible inhibitor of AChE) and 50 mM sodium phosphate buffer, pH 7.2. The rate of substrate hydrolysis by BuChE was determined by measuring the absorbance of the reaction-product at 412 nm λ.

Vma and Vmi determinations

Vma and Vmi represent two different subtypes of Vmax. The former is based on calculation of the apparent maximum activity of BuChE at a particular concentration of DHBDC along with varied concentrations of the substrate. The latter expresses the apparent maximum activity at a particular concentration of BuSCh along with varied concentrations of DHBDC.

Graphics

Graphs were plotted using GOSA (Bio-Log, Toulouse, France) and Prism (version 4; GraphPad, San Diego, CA) software and values of the correlation coefficients and specific kinetic constants were obtained by the regression analysis (linear and several different non-linear forms) computed within these packages.

Lipophilicity—clog P determinations

Computed log P (clog P) values, a measure of octanol–water partition coefficient and penetrability across membranes like the blood–brain barrier, were determined by PALLAS (CompuDrug, Sedona, AZ), and the values of specific compounds were experimentally validated. Five milliliters of 0.2 mM octanol solutions of compound was prepared, and their UV absorbencies, $A1$, were determined by spectrophotometer at 254 nm wavelength. The octanol solutions then were vigorously mixed with an equal volume of 0.1 M pH 7.0 physiological buffer for 15 min. Following separation, the absorbency of the octanol was again measured, $A2$. An octanol–water partition coefficient, P, was calculated from the formula: $P = A2/A1 - A2$.

Results

The reflective binding activity index of DHBDC for human serum BuChE at dual substrate concentrations [BuSCh; 0.6 mM (Fig. 2A) and 0.1 mM (Fig. 2B)] demonstrated the release

of DHBDC with passing reaction time. Therefore, the time required to achieve half Vmax (KT1/2) and pseudo maximum product (Pmax) were increased dramatically after 20 nM and 8 nM concentration of DHBDC at 0.6 mM and 0.1 mM concentrations of BuSCh, respectively (Fig. 2C–E). Figure 3 illustrates the relationship between the percent activity of BuChE versus the DHBDC concentration to allow calculation of an IC50 (concentration required to inhibit 50% enzymatic activity) value at each reaction time at 0.6 mM (A) and 0.1 mM (B) BuSCh concentrations. The smaller inset graphs express the new relationship of IC50 versus reaction time in this study. Determined from the studies depicted in Fig. 3, the IC50 value of DHBDC for BuChE was calculated as 3.7 to 12.2 nM at 3–25 min reaction time at a concentration of 0.6 mM BuSCh, and as 3.61–6.61 nM at 3–22 min for a 0.1 mM concentration of BuSCh (Fig. 3). New kinetic constants (NKCs) defining the interaction of the inhibitor and enzyme are presented in Table 1, and are derived from secondary replots of the primary main plots of Figs. 2 and 3 at dual concentrations of BuSCh.

A critical part in understanding how a potential inhibitor interacts with an enzyme derives from it analysis of its kinetics, which in the present study for DHBDC and BuChE was undertaken utilizing the two software packages, GOSA and Prism to gain an understanding of precise binding mechanisms, as illustrated in Fig. 4. Comparative results to define the mode of inhibition (MOI) of BuChE by our cymserine analogue are detailed in Table 2. These results were obtained by fitting the kinetic data into various built-in velocity equations in the GOSA software to determine the most appropriate equation (on the basis of the minimum value of SSE) to elucidate the mode of interaction. A sample graph for non-linear analysis for the MOI for cases #1 to #8 is illustrated in Fig. 4A, which specifically defines the activity of BuChE versus its substrate at different concentrations of DHBDC (0–16 nM). A sample graph of the linear analysis for the MOI for cases #9 to #11 is detailed in Fig. 4B. The Dixon plot for BuChE is based on reciprocal activity of the BuChE versus DHBDC concentration at different substrate concentrations. While a sample graph for linear analysis for MOI for cases #12 to #14 is provided in Fig. 4C in the form of a Lineweaver–Burk plot in which reciprocal activity of BuChE is plotted versus its reciprocal substrate concentration at different concentrations of DHBDC (0–16 nM). A Ki value of 2.22 nM was determined from an equation depicting competitive inhibition, while values of 3.24 nM and 7.91 nM were obtained for Ki1 and Ki2, respectively, from an equation defining a partial mixed type of competitive inhibition (Table 2). Secondary replots of the primary plot of Dixon (Fig. 5A) and the Lineweaver–Burk plot (Fig. 5B) of BuChE inhibition by DHBDC were constructed to differentiate between the two most plausible modes of inhibition; i.e. competitive inhibition and a partial mixed type of competitive inhibition.

Discussion

Our prior research culminated in the synthesis and characterization of the first available reversible, selective and centrally active BuChE inhibitors to elucidate the role of this enzyme in brain [3, 17, 18]. Like AChE, BuChE inactivates the neurotransmitter ACh and is a viable new therapeutic target in AD [2–4]. In healthy human brain, AChE predominates over BuChE activity (~80%:20%) [27, 28]. However, whereas AChE is localized mainly to neurons, BuChE is associated primarily with glial cells, as well as neurons. The survival of AChE −/− mice with normal levels and localization of BuChE [11] supports the concept that

BuChE has a key role that can partly compensate for the action of AChE. As both normal and AChE −/− rodents administered selective BuChE inhibitors show a time-dependent increase in brain levels of ACh [14], it is clear that both enzymes regulate brain levels of ACh. In AD, however, AChE is lost early by up to 85% in specific brain regions [13], matching the decline in ACh, whereas BuChE levels rise with disease progression [13]. The AChE to BuChE ratio thereby rises from 0.2 up to as much as 11 in cortical regions affected by AD [27, 28]. This altered ratio likely modifies the normally supportive role of BuChE from hydrolyzing excess ACh only in normal healthy brain, to too rapidly hydrolyzing already depleted levels of ACh in AD brain [2, 3]. In rats, cymserine analogs caused long-term inhibition of brain BuChE and elevated extracellular ACh levels [2, 3], and highlights an area of clinical potential for selective BuChE inhibitors [2–4].

To assess this, we recently synthesized and are pharmacologically characterizing several entirely new classes of carbamate ChEIs. These include dihydromethanobenzodioxepines [19–21], a novel series of agents that differ in their tricyclic backbone, compared to physostigmine-based ChEIs (Fig. 1). Such agents allow us to characterize the specific amino acids within AChE and BuChE through which this drug class interact. Modification of the carbamate moiety, specifically the use of a 4′-isopropyl-phenylcarbamate, provides a high selectivity for BuChE inhibitory action in the form of the compound, DHBDC [19].

Assessment of the apparent binding activity index of DHBDC for human serum BuChE at dual substrate concentrations provides a measure of enzyme/inhibitor tightness in a concentration- and time-dependent manner (Fig. 2). The basis of the Ellman technique [22] that underpins our analysis is that molecules of free BuChE with an open (unihibited) active site are able to react with substrate, BuSCh, to hydrolyze it into butyrate and thiocholine. The latter then reacts with DTNB to form a color reaction-product in a time-dependent manner (zero inhibitor concentration curves in Fig. 2A and B for 0.6 mM and 0.1 mM substrate (BuSCh), respectively). As illustrated in Fig. 2(C and D), the time required to achieve half Vmax (KT1/2) and the pseudo maximum product (Pmax) were increased dramatically around 20 nM and 8 nM concentrations of DHBDC at 0.6 mM and 0.1 mM concentrations of BuSCh, respectively. This was consequent to the linearity of the primary profiles with increasing DHBDC concentration present in the main plot (Fig. 2A and B). At a higher substrate concentration (0.6 mM), where a dominant enviorement of BuSCh molecules are available for enzyme interaction, a greater concentration of inhibitor (20 nM) is required to induce a dramatic increase in KT1/2 and Pmax (Fig. 2C and D). By comparison, at a lower BuSCh concentration (0.1 mM), an 8 nM inhibitor concentration provides a critical dose to increase the parameters, KT1/2 and Pmax. This is reflected in Table 1; wherein, the calculated kinetic constants are clearly substrate concentration-dependent.

In our original description of the synthesis of novel anticholinesterases based on the molecular skeleton of methanobenzodioxepine [19], an initial simple enzyme kinetic analysis of the derived inhibitors was undertaken at half-log concentration steps between 0.3 nM and 10 μM utilizing a single substrate concentration (0.5 mM) and reaction time (30 min). This allowed the determination of a general comparative IC50 value for inhibition of human plasma BuChE, and compound **12**, DHBDC, with an IC50 of 22 ± 5 nM [19] was

chosen for further analysis consequent to its potency for BuChE vs. AChE (IC50 4300 ± 350 nM) and 195-fold selectivity. In the current study, however, undertaking a more precise (concentration range 2.4–40 nM) and indepth (dual substrate and multiple time) analysis a lower IC50 value, commensurate with greater potency, was determined—particularly in the presence of a lower substrate concentration (0.1 mM) (Fig 3A and B). A new relationship between IC50 versus reaction time (Fig. 3 insets) predicts the reversible nature of the inhibition of BuChE by DHBDC.

In addition to the design and synthesis of new and potent BuChE and AChE selective inhibitors as potential therapeutics, a driving rationale behind our creation of methanobenzodioxepine carbamates was their utility as tools to elucidate the binding interactions between the cholinesterases enzymes and the classic carbamates based on the tricyclic hexahydropyrroloindole backbone of physostigmine [19, 21]. Physostigmine has served as a template in the development of several agents for AD, including a slow-release formulation of the parent compound (synapton, Forest Laboratories, St Louis, MO), its heptyl-carbamate (eptylstigmine, Mediolanum, Italy), both withdrawn from clinical development due to efficacy/toxicity issues, and the phenyl-carbamate, phenserine (National Institute on Aging, Baltimore, MD, and TorreyPines Therapeutics Inc., San Diego, CA) (Fig. 1C) in development for mild to moderately afflicted AD patients [29].

The catalytic subunits of BuChE and AChE have a molecular mass of 60–80 kDa, depending on their level of glycosylation and the species from which they derive [1, 27]. The active site for ACh hydrolysis is buried within a primarily hydrophobic gorge of some 20 Å deep within each [27, 30, 31]. In their interaction and inhibition of BuChE and AChE, it is generally believed that, under physiological conditions, the basic N1(CH3) group of physostigmine (P*K*a = 8.46 [17]) and analogues, including pyridostigmine, gains a H+ to generate a charged quaternary ammonium group. Kinetic analysis of cationic ligands has shown that the active site of the enzymes, and in particular AChE, have a large negative charge [32], thus creating a strong dipole along the active site gorge [33]. In a manner similar to the charged choline moiety of ACh, positively charged physostigmine and analogues likely are drawn into the enzyme by electrostatic field forces. Thereafter, such inhibitors interact with specific binding domains to form an inhibitor–enzyme complex. Whereas the quaternary ammonium group plays an important role in this process, carbamate inhibitors such as DHBDC possess a tricyclic backbone that is uncharged, consequent to the replacement of basic nitrogens with neutral oxygens [19, 21] (Fig. 1). As demonstrated in the present study, the compound nevertheless retains a potent inhibitory activity.

This phenomenon can be potentially explained by the fact that the “anionic” site of BuChE and AChE are lined with hydrophobic residues, consequent to the presence of tryptophan and tyrosine that support the opportunity for hydrophobic interactions [34]. Our recent molecular modeling analysis of this interaction suggests a π-π or lipophilic (C–H–π) interaction system of the tricyclic backbone of the inhibitor and the indole system of Trp82 of human BuChE [21] (or Trp86 in human AChE for AChE-selective carbamates of the dihydrobenzodioxepine series) [32].

The Kiapp and a predicted Ki for the selective BuChE-I, bisnorcymserine, have been reported as 0.7 nM and 0.131 nM respectively [23]. Whereas in the case of cymserine, these values are 115 and 38 nM, respectively [24]. By comparison, the estimated Ki value for DHBDC in the current study is 2.22 nM, according to the competitive inhibition equation, or 3.24 nM and 7.91 nM for Ki1 and Ki2, respectively, according to the partial mixed type of competitive inhibition equation (Table 2). DHBDC is less potent than bisnorcymserine but more than cymserine. As plasma levels of the close analogue, phenserine, reached 1.95 ng/ml (5.79 nM) at a well tolerated dose of 10 mg in humans [35], we predict that the estimated Ki value for DHBDC will lie within a clinically achievable range, particularly since cymserine analogues are better tolerated than phenserine in preclinical models and thus can be administered in higher doses [19].

The reason for selecting the partial mixed or partial competitive inhibition mode (Fig 4A) for BuChE inhibition by DHBDC, from the comparative possible scenarios described in Table 2 for non-linear analysis cases #1 to #8, was based on the ‘sum of the squared error’ (SSE) values (a measure of the fit of our data to the equation, whose minimum was 1.82 in cases #1 to #8). By contrast, in the category of linear analysis cases #9 to #14, a lower SSE minimum value (0.042) was obtained for a competitive mode of inhibition. The interaction of DHBDC with BuChE can be understood through following Scheme 1.

In accord with this, the secondary slope replots of the primary plot of Dixon in Fig. 5A closely resembles a classical plot for competitive inhibition in which the replot line goes through the origin (0 XY value). For our inhibitor, however, X- and Y-axis intercept values were 0.156 and −0.00095, respectively. To further define the potential mode of action, a secondary slope replot of the primary Lineweaver–Burk plot of BuChE inhibition by DHBDC was undertaken (Fig. 5B) to provide reciprocal Kmapp (Kma) and Vmaxapp (Vma) replots and differentiate between competitive inhibition and a mixed type of competitive inhibition. The parameter 1/Vma should significantly increase in the latter case; however, it was found to be close to flat (slope of −0.00124), again reflecting that inhibition was more of a competitive type in the current study. However, the described slight divergence regarding the slope intercept (Fig. 5A) and 1/Vma (Fig. 5B) sugests the potential of a minor mixed component. Hence, the part of Scheme 1 that belongs to a mixed type of competitive inhibition is, accordingly, shaded.

In synopsis, DHBDC represents an interesting and potent BuChE-selective inhibitor that possesses IC50, Ki and related kinetic parameters that are likely attainable in humans, and the current study provides target concentrations to focus initial clinical trials. Interestingly, the replacement of both indole nitrogen moieties in the tricyclic hexahydropyrroloindole backbone common to the experimental AD drug, phenserine, and its BuChE-selective analogues, cymserine and bisnorcymserine, by neutral oxygen moieties changes the mode of action to a competitive inhibition from a non-competitive oriented type [23–26]. This structural modification also provides additional lipophilicity to augment permeability at biological structures, such as the blood-brain barrier (Fig. 1. clog P values). A recent study by Pepeu and colleagues [36] in rodents suggests that equivalent selective inhibition of either BuChE or AChE separately (achieved by a cymserine analogue and donepezil, respectively), or their co-inhibition by a non-selective ChE-I (achieved by rivastigmine)

result in similar elevations in brain ACh, although BuChE accounts for only 10% of total brain cholinesterase activity whereas AChE account for 90%. Whether or not selective BuChE inhibition could accomplish such elevations of brain ACh in AD remains unknown as, to date, clinical assessment of a selective reversible BuChE-I has yet to be undertaken in humans. Clinical drug candidates are, however, now available to assess whether or not their significant promise in preclinical models does, indeed, translate and it is hoped that such a study could soon be initiated with an agent such as DHBDC.

Acknowledgments

This research was supported in part by the Intramural Research Program of the National Institute on Aging, National Institutes of Health.

Abbreviations

ACh	Acetylcholine
AChE	Acetylcholinesterase
AChE-Is	Acetylcholinesterase inhibitors
AD	Alzheimer's disease
BuChE	Butyrylcholinesterase
BuSCh	Butyrylthiocholine iodide
BuChE-Is	Butyrylcholinesterase inhibitors
ChEs	Cholinesterases
ChEIs	Cholinesterase inhibitors
CNS	Central nervous system
DHBDC	Dihydrobenzodioxepine cymserine (4,5-dihydro-2,5-methyl-1,3-benzodioepin-7-yl N-(4′-isopropylphenyl)-carbamate)
KT50	Concentration of inhibitor doubles KT1/2
PPC	Concentration of inhibitor doubles pseudo Pmax
KT1/2	Time required for half Vmax
RI	Rate of IC50
RβA	Reflective binding activity

References

1. Darvesh S, Hopkins DA, Geula C. Neurobiology of butyrylcholinesterase. Nat Rev Neurosci. 2003; 4:131–138. [PubMed: 12563284]
2. Greig NH, Lahiri DK, Sambamurti K. Butyrylcholinesterase: an important new target in Alzheimer's disease therapy. Int Psychogeriatrics. 2002; 14:77–91.

3. Greig NH, Utsuki T, Ingram DK, et al. Selective butyrylcholinesterase inhibition elevates brain acetylcholine, augments learning and lowers Alzheimer β-amyloid peptide in rodent. Proc Natl Acad Sci USA. 2005; 102:17213–17218. [PubMed: 16275899]
4. Ballard CG, Greig NH, Guillozet-Bongaarts AL, et al. Cholinesterases: roles in the brain during health and disease. Curr Alzheimer Res. 2005; 2:281–290. [PubMed: 15974893]
5. Farlow MR, Cummings JL. Effective pharmacologic management of Alzheimer's disease. Am J Med. 2007; 120:388–397. [PubMed: 17466645]
6. Cummings JL. Alzheimer's disease. N Engl J Med. 2004; 351:56–67. [PubMed: 15229308]
7. Silver, A. The biology of cholinesterases. Elsevier; Amsterdam: 1974.
8. De Vriese C, Gregoire F, Lema-Kisoka R, et al. Ghrelin degradation by serum and tissue homogenates: identification of the cleavage sites. Endocrinology. 2004; 145:4997–5005. [PubMed: 15256494]
9. Darvesh S, Grantham DL, Hopkins DA. Butyrylcholinesterase in normal human amygdala and hippocampal formation. J Comp Neurol. 1998; 393:374–390. [PubMed: 9548556]
10. Darvesh S, Hopkins DA. Differential distribution of butyrylcholinesterase and acetylcholinesterase in the human thalamus. J Comp Neurol. 2003; 463:25–43. [PubMed: 12811800]
11. Mesulam M-M, Guillozet A, Shaw P, et al. Acetylcholinesterase knockouts establish central cholinergic pathways and can use butyrylcholinesterase to hydrolyze acetylcholine. Neuroscience. 2002; 110:627–639. [PubMed: 11934471]
12. Mesulam M-M, Guillozet AL, Shaw P. Widely spread butyrylcholinesterase can hydrolyze acetylcholine in the normal and Alzheimer brain. Neurobiol Dis. 2002; 9:88–93. [PubMed: 11848688]
13. Perry EK, Perry RH, Blessed G. Changes in brain cholinesterases in senile dementia of Alzheimer type. Neuropathol Appl Neurobiol. 1978; 4:273–277. [PubMed: 703927]
14. Hartmann J, Kiewert C, Duysen EG, et al. Excessive levels of hippocampal acetylcholine in acetylcholinesterase-knockout mice are moderated by butyrylcholinesterase activity. J Neurochem. 2007; 100:1421–1428. [PubMed: 17212694]
15. Guillozet AL, Smiley JF, Mash DC, et al. Butyrylcholinesterase in the life cycle of amyloid plaques. Ann Neurol. 1997; 42:909–918. [PubMed: 9403484]
16. Diamant S, Podoly E, Friedler A, et al. Butyrylcholinesterase attenuates amyloid fibril formation in vitro. Proc Natl Acad Sci USA. 2006; 103:8628–8633. [PubMed: 16731619]
17. Greig NH, Pei X-F, Soncrant T, et al. Phenserine and ring-C hetero-analogues: drug candidates for the treatment of Alzheimer's disease. Med Chem Rev. 1995; 15:3–31.
18. Yu QS, Holloway HW, Utsuki T, et al. Phenserine-based synthesis of novel selective inhibitors of butyrylcholinesterase for Alzheimer's disease. J Med Chem. 1999; 42:1855–1861. [PubMed: 10346939]
19. Luo X, Yu QS, Zhan M, et al. Novel anticholinesterases based on the molecular skeletons of furobenzofuran and benzodioxepine. J Med Chem. 2005; 48:986–994. [PubMed: 15715468]
20. Luo W, Yu QS, Holloway HW, et al. Syntheses of tetrahydrofurobenzofurans and dihydro-methanobenzodioxepines from 5-hydroxy-3-methyl-3H-benzofuran-2-one. Re-arrangement and ring expansion under reductive conditions on treatment with hydrides. J Org Chem. 2005; 70:6171–6176. [PubMed: 16050674]
21. Luo W, Yu QS, Kulkarni SS, et al. (−) And (+)-*o*-carbamoyl phenols of pyrroloindole, furoindole, furobenzofuran and benzodioxepine: enantiomeric syntheses and structure/activity relationship for human acetyl- and butyrylcholinesterase inhibitory action. J Med Chem. 2006; 49:2174–2185. [PubMed: 16570913]
22. Ellman GL, Courtney KD, Andres V Jr, et al. A new and rapid colorimetric determination of acetylcholinesterase activity. Biochem Pharmacol. 1961; 7:88–95. [PubMed: 13726518]
23. Kamal MA, Yu Q-S, Holloway HW, et al. Kinetics of human serum butyrylcholinesterase and its inhibition by a novel experimental Alzheimer therapeutic, bisnorcymserine. J Alzheimers Dis. 2006; 10:43–51. [PubMed: 16988481]
24. Kamal MA, Al-Jafari AA, Yu Q-S, et al. Kinetic analysis of the inhibition of human butyrylcholinesterase with cymserine. Biochim Biophys Acta. 2006; 1760:200–206. [PubMed: 16309845]

25. Al-Jafari AA, Kamal MA, Greig NH, Alhomida AS, Perry EK. Kinetics of human erythrocyte acetylcholinesterase inhibition by a novel derivative of physostigmine: Phenserine. Biochem Biophys Res Commun. 1998; 248:180–185. [PubMed: 9675107]

26. Al-Jafari AA, Kamal MA, Alhomida AS, et al. Kinetics of rat brain acetylcholinesterase inhibition by two experimental Alzheimer's disease drugs, phenserine and tolserine. J Biochem Mol Biol Biophys. 2000; 4:323–335.

27. Giacobini, E. Butyrlcholinesterase: its function and inhibitors. Martin Dunitz; London and New York: 2003.

28. Giacobini E. Cholinesterases: new roles in brain function and in Alzheimer's disease. Neurochem Res. 2003; 28:515–522. [PubMed: 12675140]

29. Greig NH, Sambamurti K, Yu Q-S, et al. An overview of phenserine tartrate, a novel acetylcholinesterase inhibitor for the treatment of Alzheimer's disease. Curr Alzheimer Res. 2005; 2:281–291. [PubMed: 15974893]

30. Soreq, H.; Zakut, H. Human cholinesterases and anticholinesterases. Academic Press; New York: 1993.

31. Sussman JL, Harel M, Frolow F. Atomic structure of acetylcholineesterase from *Torpedo californica*: a prototypic acetylcholine-binding protein. Science. 1991; 253:872–879. [PubMed: 1678899]

32. Nolte HJ, Rosenberry TL, Neumann E. Effective charge on acetylcholinesterase active sites determined from the ionic strength dependence of association rate constants with cationic ligands. Biochemistry. 1980; 19:3705–3711. [PubMed: 7407068]

33. Ripoll DR, Faerman CH, Axelsen PH, et al. An electrostatic mechanism for substrate guidance down the aromatic gorge of acetylcholinesterase. Proc Natl Acad Sci USA. 1993; 90:5128–5132. [PubMed: 8506359]

34. Koellner G, Steiner T, Millard CB, et al. A neutral molecule in a cation-binding site: specific binding of a PEG-SH to acetylcholinesterase from *Torpedo californica*. J Mol Biol. 2002; 320:721–725. [PubMed: 12095250]

35. Greig NH, Ruckle J, Comer P, et al. Anticholinesterase and pharmacokinetic profile of phenserine in healthy elderly human subjects. Curr Alzheimer Res. 2005; 2:483–492. [PubMed: 16248851]

36. Cerbai F, Giovannini MG, Melani C, et al. N(1)-Phenethyl-norcymserine, a selective butyrylcholinesterase inhibitor, increases acetylcholine release in rat cerebral cortex: A comparison with donepezil and rivastigmine. Eur J Pharmacol. 2007 Epub ahead of print on pubmed.

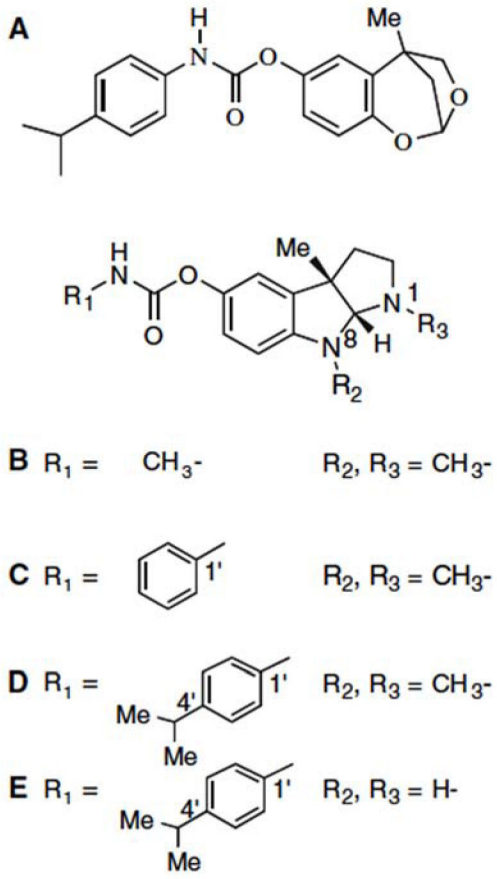

Fig. 1.

Chemical structures of (**A**) dihydrobenzodioxepine cymserine (DHBDC) (clog *P* value 4.58), (**B**) (−)-physostigmine. (**C**) (−)-phenserine (clog *P* value 2.22), (**D**) (−)-cymserine (clog *P* value 3.51) and (**E**) (−)-bisnorcymserine (clog *P* value 1.80)

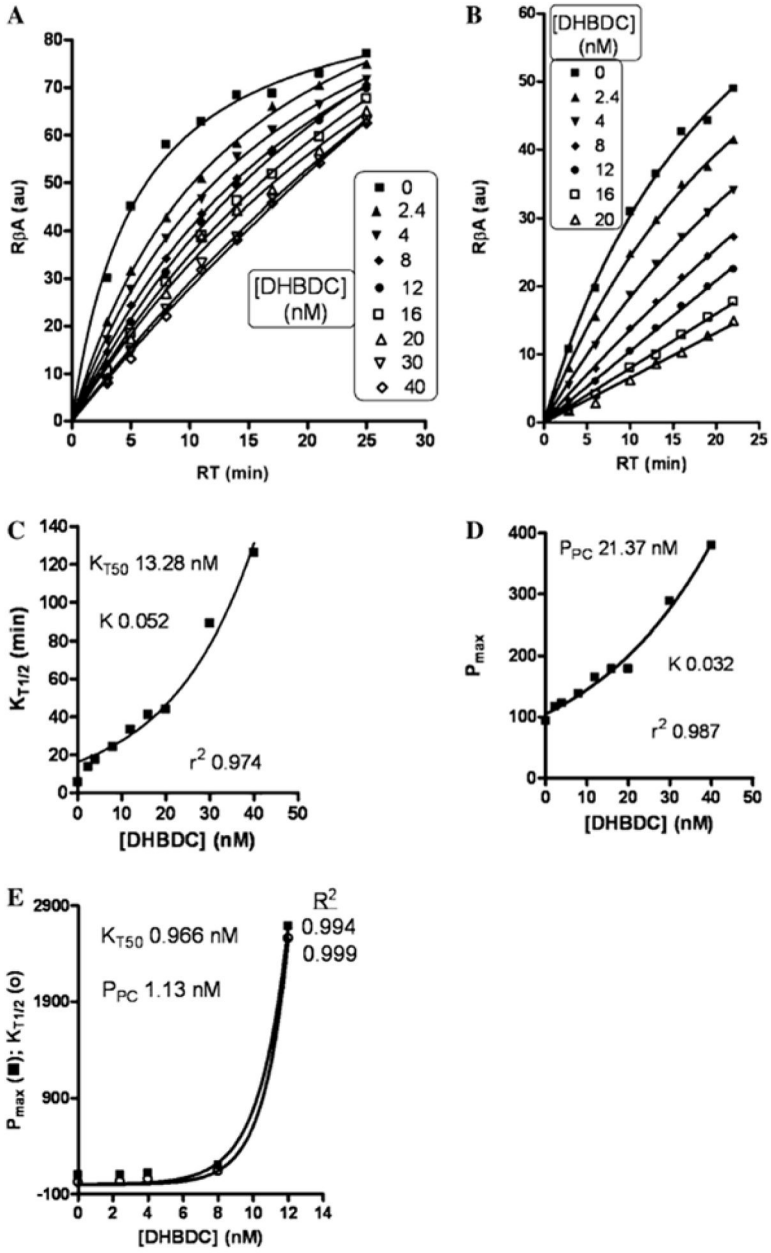

Fig. 2.

Tightness of bound DHBDC with BuChE at 0.6 mM (**A**) and 0.1 mM (**B**) BuSCh: main plots demonstrate reflective binding activity versus reaction time; **C** and **D** are secondary replots of primary main plot of A, while **E** is the secondary replot of primary main plot of B. (R2 in case of A for 0, 2.4, 4, 8, 12, 16, 20, 30 and 40 nM of DHBDC was found as 0.987, 0.998, 0.999, 0.999, 0.998, 0.998, 0.992, 0.998 and 0.998, respectively)

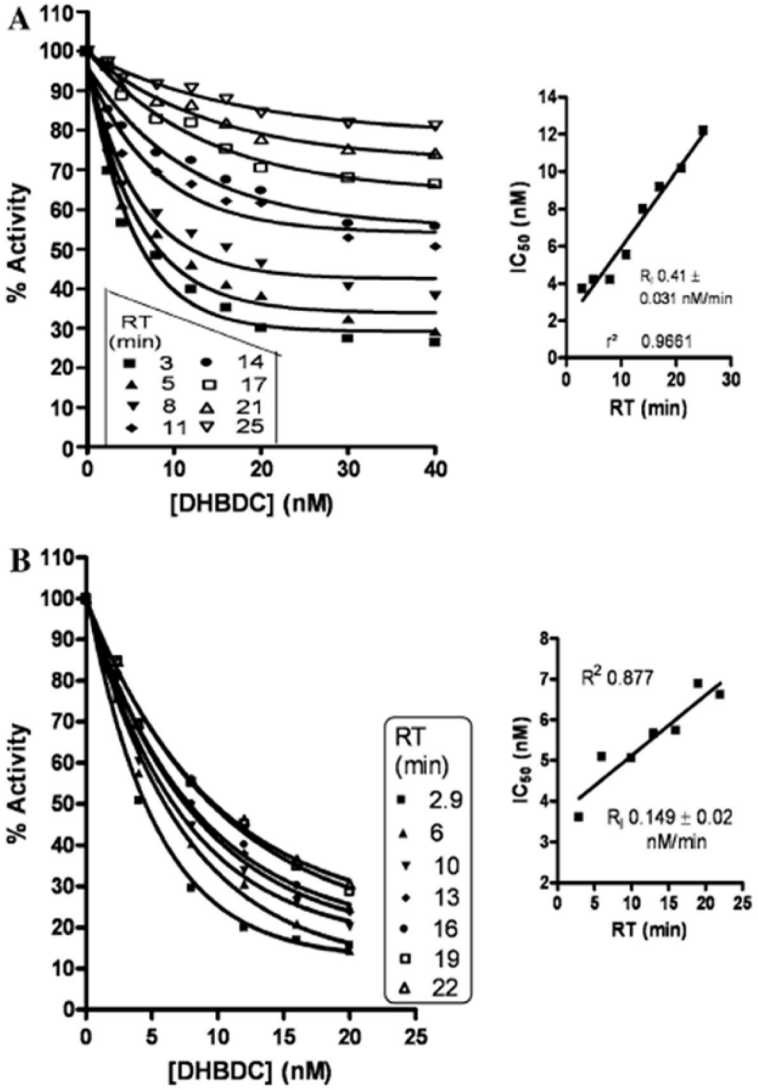

Fig. 3.

Demonstration of percent activity of BuChE versus DHBDC concentration to calculate the IC50 at each reaction time at 0.6 mM (**A**) and 0.1 mM (**B**) BuSCh. Inset: Demonstration of IC50 versus reaction time. (R2 in case of A for 3, 5, 8, 11, 14, 17, 21 and 25 min reaction time was found as 0.982, 0.967, 0.961, 0.939, 0.965, 0.981, 0.980 and 0.973, respectively).

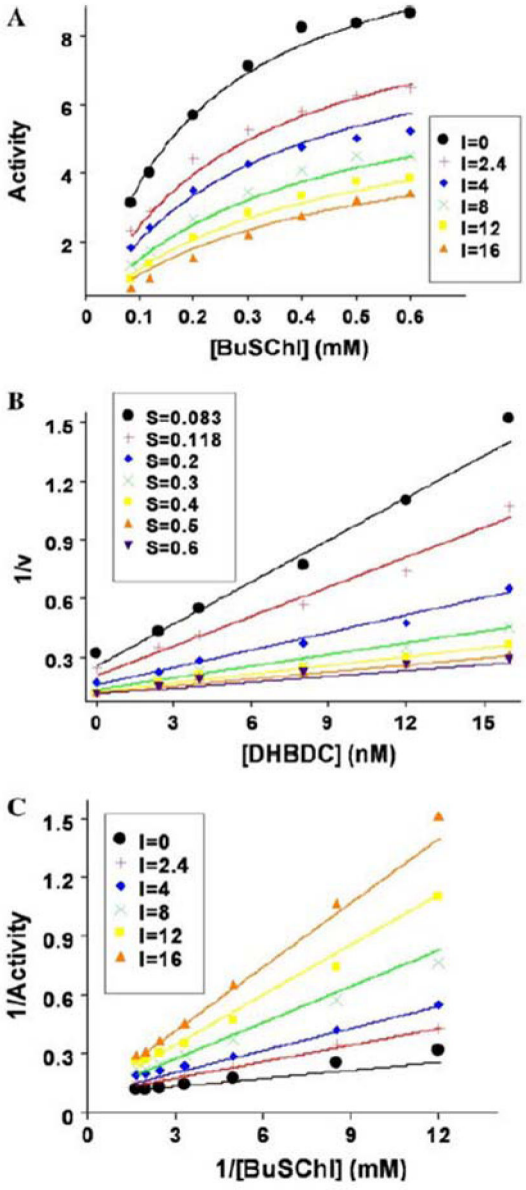

Fig. 4.

Kinetic study of BuChE: (**A**) BuChE activity versus its substrate at different concentrations of DHBDC, as described in the legend box. (**B**) Dixon plot for BuChE reciprocal activity versus DHBDC concentration at different substrate concentrations, as described in the legend box. (**C**) Lineweaver-Burk plot of BuChE reciprocal activity versus its reciprocal substrate concentration at different concentrations of DHBDC, as detailed in the legend box

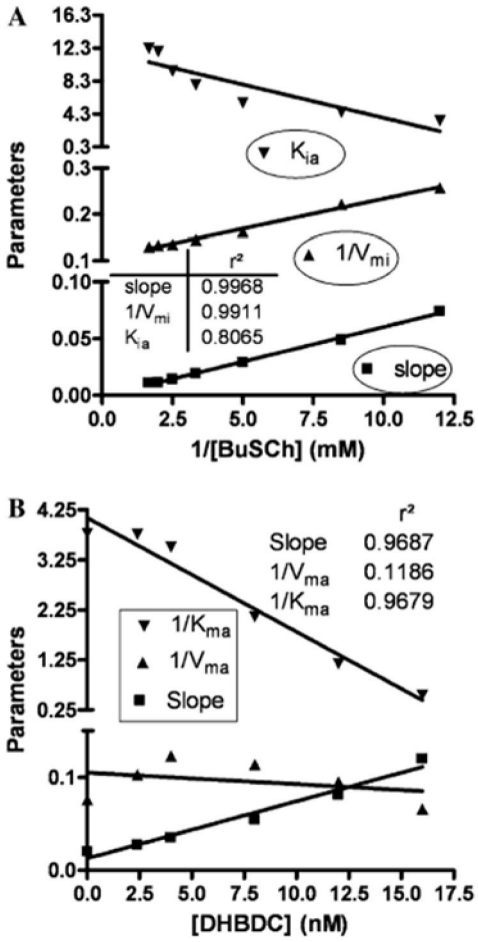

Fig. 5.

Secondary replots of primary plot of Dixon (**A**) and Lineweaver-Burk (**B**) plot of BuChE inhibition by DHBDC

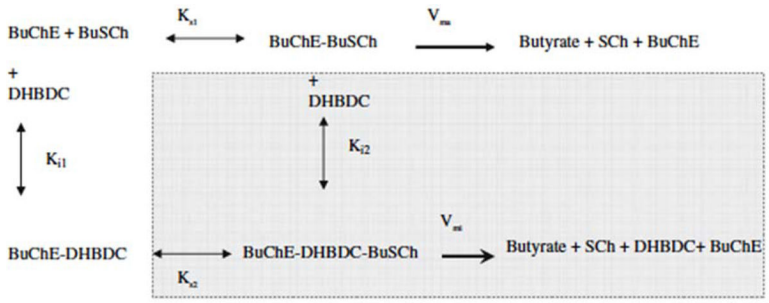

Scheme 1.

A possible presentation for the expression of competition between substrate (BuSCh) and an inhibitor (DHBDC) to bind with an enzyme (BuChE) in this current study

Table 1

New kinetic constants (NKC) at dual concentrations of BuSCh

NKC	BuSCh (0.6 mM)	BuSCh (0.1 mM)
K_{T50} (nM)	13.28	0.966
P_{PC} (nM)	21.37	1.13
R_1 (nM/min)	0.41 ± 0.031	0.149 ± 0.02

P_{PC} concentration of inhibitor to double pseudo P_{max}; K_{T50}, concentration of inhibitor to double $K_{T1/2}$; R_1, rate of IC_{50}

Table 2

Comparative results for mode of inhibition (MOI) of BuChE by dihydrobenzodioxepine cymserine

Number	*MOI*	K_m (mM)	k_{cat} (au)	K_i or K_{i1} (*) (nM)	k_{i2} (nM)	α	*SSE*
1	*CI*	*0.167 ± 0.042*	*10.70 ± 0.91*	*2.48 ± 0.5*	–	–	*4.03*
2	*NCI*	*0.273 ± 0.05*	*12.98 ± 1.04*	*7.87 ± 0.76*	–	–	*3.41*
3	*UCI*	*0.419 ± 0.15*	*15.64 ± 3.2*	*3.84 ± 0.99*	–	–	*9.67*
4	*MI*	*0.208 ± 0.05*	*11.65 ± 1.01*	*4.33 ± 1.45**	*14.67 ± 7.1*	–	*2.62*
5	*PCI*	*0.214 ± 0.04*	*12.01 ± 0.9*	*3.24 ± 0.95**	*7.91 ± 2.9*	*0.224 ± 0.09*	*1.82*
6	*PNC*	*0.275 ± 0.042*	*13.29 ± 0.94*	*5.05 ± 1.2*	–	*0.152 ± 0.06*	*2.495*
7	*PUCI*	*0.42 ± 0.16*	*15.64 ± 3.2*	*3.84 ± 1.16*	–		*9.67*
8	*PM*	*0.214 ± 0.04*	*12 ± 0.9*	*3.24 ± 0.95**	*7.91 ± 2.97*	*0.224 ± 0.09*	*1.82*
9	*DplCI*	*0.146 ± 0.057*	*10.42 ± 1.87*	*2.34 ± 0.66*	–	–	*0.042*
10	*DplNCI*	*0.382 ± 0.12*	*15.2 ± 4.06*	*6.48 ± 1.58*	–	–	*0.157*
11	*DplUCI*	*0.624 ± 1.13*	*15.2 ± 23.9*	*3.21 ± 5.96*	–	–	*0.967*
12	*LBplCI*	*0.146 ± 0.057*	*10.42 ± 1.87*	*2.34 ± 0.66*	–	–	*0.042*
13	*LBplNCI*	*0.382 ± 0.12*	*15.2 ± 23.93*	*6.49 ± 1.58*	–	–	*0.157*
14	*LBplUCI*	*0.624 ± 1.13*	*15.2 ± 23.93*	*3.21 ± 5.96*	–	–	*0.967*

C, competitive; D, Dixon; LB, Lineweaver-Burk; I, inhibition; M, mixed; N, noncompetitive; P, partial; pl, plot; U, uncompetitive; SSE, sum of squared errors

* refers to Ki1 value